Radio-mechanical Characterization of Epidermal Antennas during Human Gestures

C. Miozzi, *Student Member, IEEE*, G. Diotallevi, M. Cirelli, *Student Member, IEEE*, P. P. Valentini, G. Marrocco, *Member, IEEE*

***Abstract*— Recent developments in Materials and Radiofrequency Identification (RFID) technologies are currently boosting the development of new class of flexible and elastic epidermal devices for the wireless remote monitoring of biophysical parameters. As tightly bio-integrated with the skin, epidermal antennas are subjected to mechanical deformation during the natural movements and gestures of the human body. The experienced effect is a degradation of the communication performance of the RFID link. In this contribution, we evaluate the stiffness and the change of the radiation gain of on-skin UHF antennas in common gestures by a combined mechanical-electromagnetic model to provide a database and a modelling methodology to improve the design of deformation-tolerant skin antennas. The deformation of the skin is firstly quantified by using a contactless 3D scanner and then the communication impact is predicted by means of an electromagnetic analysis of stretched antennas for some relevant cases of thin-wire layouts. Preliminary numerical simulations and experimentations demonstrated that constraints over low stiffness and insensitivity of radiation gain could be not always compatible. An epidermal antenna may undergo up to 3-4 dB of gain degradation that converts to 30% reduction of the read distance for the strain orientation producing the minimum mechanical stiffness. The derived deformation database could be useful to improve the design of more robust epidermal antennas.**

***Index Terms*—Epidermal Electronics, Radiofrequency Identification.**

I. Introduction

The current trend of pervasive and personal monitoring of the human health and wellness is quickly stimulating the shift of electronics from wearable clothes and accessories to a direct assembly over the skin, according to the paradigm of Epidermal Electronics [1]. Flexible biocompatible and breathable membranes hosting sensors, microchip transponders and antennas can be stuck over the epidermis to collect biophysical parameters with a high comfort for the user [2], [3]. Usually, epidermal devices communicate through the backscattering modulation [4], [5] with a remote interrogator within the Radiofrequency Identification (RFID) framework. Among some options (NFC, HF, UHF), the UHF (860-960 MHz) standard [6], [7] potentially enables a superior read distance of 0.5-2 m so that a user can be monitored and tracked as he crosses a gate [8] as well as he moves within small environments. Achieving a stable and robust communication performance when an antenna is put onto the skin is still a technology challenge due to the high electrical loss of the tissues and to the extreme variability of the human body in terms of shape and tissue layering [9]. Moreover, epidermal devices are continuously subjected to mechanical stress during natural body gestures, like turning the neck and lifting an arm that could also modify their electromagnetic response, namely their input resistance and gain and, overall, the read distance. Moreover, depending on the technology that is used to deploy the conductor onto the holding membrane, the fatigue produced by the natural gestures may provoke a damage of the device. For instance, Fig. 1a shows an example of UHF epidermal thermometer [10] (whose layout will be better described later on) that was fabricated by using a very thin (80 μm diameter) conducting copper wire, deployed onto a medical-grade elastomer. After three days of wearing on the arm, the wire path was broken (Fig. 1b) thus preventing the wireless reading of the data.

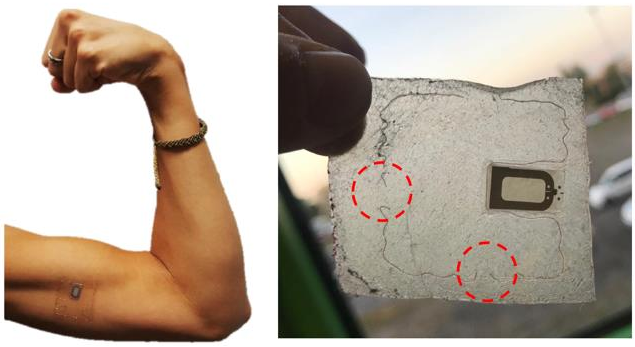

a) b)

Fig. 1: Fatigue and damaging: stretchable thin wire UHF antenna a) just placed on the skin and b) after three days of wearing in daily activities.

Mechanical-robust circuit layouts have been already deeply investigated [1] to absorb deformation, thus reducing the mechanical stress. Optimal configurations include meander-like paths and this strategy has been successfully applied for HF circuits and antennas. However, when moving to the UHF band, on-skin meander-line antennas are less effective due to the power loss induced by the transmission line current modes that

All authors are with the University of Rome Tor Vergata, Via del Politecnico 1, 00133, Roma (IT) (corresponding author to provide phone: (+39)0672597335; e-mail: carolina.miozzi@uniroma2.it).

An earlier version of this paper was presented at the *IEEE International Conference on Flexible and Printable Sensors and Systems* (FLEPS) and was published in its Proceedings. DOI: 10.1109/FLEPS.2019.8792315.

do not contribute to radiation while instead dissipate power into the human body, thus worsening the radiation efficiency.

Although the deformation (mostly bending) of UHF and microwave antennas over textiles is a well-studied topic [11], what happens at UHF frequencies with on-skin antennas due to the natural stretching of the body is instead - to the best of our knowledge - not yet investigated.

This contribution, extending the preliminary results in the conference paper [12], presents a numerical campaign aimed at quantifying the maximum deformation of human skin in several parts of the body during natural gestures. The overall purpose is to provide a database and a modelling methodology to improve the design of deformation-tolerant skin antennas. The methodology involves the use of a contactless 3D scanner and mechanical modelling (Section II). The reconstruction of simplified biomechanical models through the paradigm of the reverse engineering is then applied to the evaluation of the mechanical strain and stress of typical epidermal antennas. The effect of such deformation on the communication performance of the antenna is hence derived (Section III) by means of an electromagnetic model. A combined radio-mechanical representation of the stretched antenna w.r.t. unstretched one is then proposed. Finally, the simulated results are corroborated by some experimental measurements of a manufactured antenna placed on the body (Section IV).

II. Digitalization of Skin Stretching

The effect of skin deformation during natural gestures generates a stretching/shrinking of the skin, as well as a change of the surface curvatures. The main problem in the assessment of the deformation is that skin movements are large and three-dimensional. Moreover, a direct measurement of skin shape using a contact probe may alter the local deformation of the tissues. For this reason, the investigation is based on the digitalization of the anatomic segments using a contactless scanner and a semi-automatic procedure able to extract deformation parameters that are useful to derive the corresponding electromagnetic response. The next discussed procedure will be applied to the analysis of four body parts with several common gestures, as in Fig. 2.

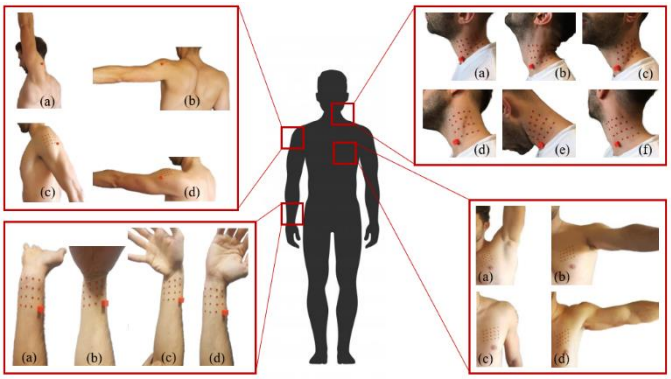

Fig. 2: Gestures considered for four body parts of interest.

A. Digitalization of skin

A professional handheld 3D scanner (Artec Eva) was used to capture and digitalize the shape of the skin during natural gestures without contact. The information is then processed to extract stretching parameters. A control grid of spherical ($r = 0.5$ mm) plastic markers $\mathrm{M}_{i,j}$ and a reference cube ($l = 5$ mm) were applied on the considered skin portion to track the location of relevant points on the surface (see the example of neck in Fig. 3). The scanner is able to compute the coordinates of each point on the skin and the cube is used to provide a rigid reference frame to map the deformations over a rigid motion. When a gesture occurs, each control grid node, initially at $\mathrm{M}^0_{i,j}$, moves to $\mathrm{M}_{i,j}$, subjected to a rigid motion plus a local displacement. The rigid motion is due to the whole body movement and the local displacement is due to the skin deformation. In order to compute the local displacement $\mathrm{M}^D_{i,j}$, its rigid motion $\mathrm{M}^{RM}_{i,j}$ (with respect to the reference cube) is subtracted to the whole displacement $\mathrm{M}_{i,j}$, acquired by the scanner:

$$\mathrm{M}^D_{i,j} = \mathrm{M}_{i,j} - \mathrm{M}^{RM}_{i,j} \tag{1}$$

The skin surface S is then interpolated through the coordinates $\mathrm{M}^D_{i,j}$ by means of NURBS surfaces [13] to have continuous functions over the entire region which is defined by two scalar parameters u and v spanning the two main directions $(u \quad v) \rightarrow \mathrm{S}(u \quad v)$ (Fig. 3). In the same way, the coordinates $\mathrm{M}^0_{i,j}$ are interpolated to get the undeformed surface skin S^0. Thanks to the closed-form representations, for each point $\mathrm{P}(u \quad v)$ of the surface S, the actual nonlinear strain ε along the three relevant directions (first and second principal u and v and diagonal t) can be computed as [14]:

$$\begin{aligned}
\varepsilon_u\big(P(u \quad v)\big) &= ln\left(\frac{\left\|\frac{dS}{du}\right\|}{\left\|\frac{dS^0}{du}\right\|}\right)\\
\varepsilon_v\big(P(u \quad v)\big) &= ln\left(\frac{\left\|\frac{dS}{dv}\right\|}{\left\|\frac{dS^0}{dv}\right\|}\right)\\
\varepsilon_t\big(P(u \quad v)\big) &= ln\left(\frac{\left\|\frac{dS}{dt}\right\|}{\left\|\frac{dS^0}{dt}\right\|}\right)
\end{aligned} \tag{2}$$

where $\frac{dS}{dt} = \nabla S \cdot \hat{\underline{t}}$ and $\nabla S = \left\{\frac{dS}{du} \quad \frac{dS}{dv}\right\}^{\boldsymbol{T}}$. This evaluation is represented in a colour vector stretching map (Fig. 4) that depicts the strain of relevant points over the space of $(u \quad v)$ parameters using different colours. The deformation maps of all the considered gesture of a same body region (Fig. 5a) are finally compressed in a meta-representation of (Fig. 5b) where the overall strain module $|\varepsilon|$ is obtained as the maximum values among the considered cases. For this purpose, the thickness of the mesh lines represents the maximum intensity of deformation along that direction. The example of neck mainly shows an elongation up to almost $\varepsilon = 0.3$ for the vertical and diagonal directions, while the horizontal one is subjected to a lower stretch. Fig. 6 finally summarizes the meta-

representations of the strain for all the considered body regions and gestures as in Fig. 2.

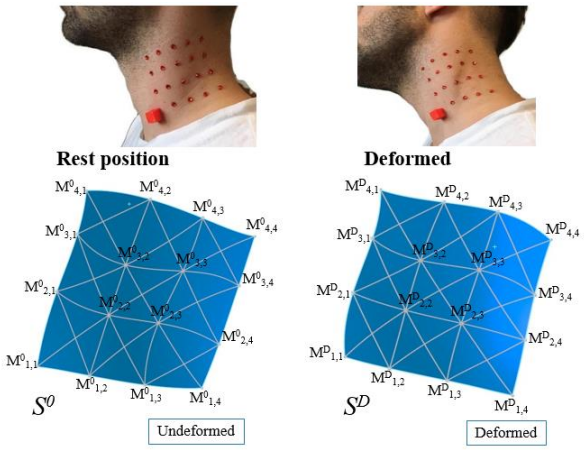

Fig. 3: Digitalization of skin deformation by means of an array of optical markers and 3D NURBS interpolation (spline).

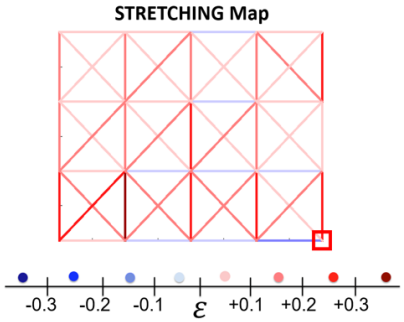

Fig. 4: Example of coloured deformation map of the skin strain over a fixed triangular grid in the case of neck movement, as in Fig. 3.

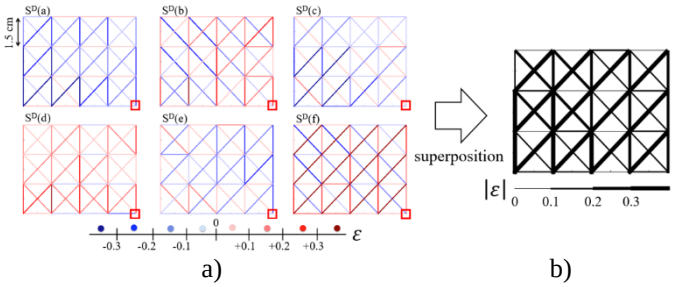

Fig. 5: a) Representation of the deformation of the neck skin during the six gestures in Fig. 2. b) Compressed meta-representation of all the cases so that the thickness of the mesh lines is proportional to the maximum strain module $|\boldsymbol{\varepsilon}|$.

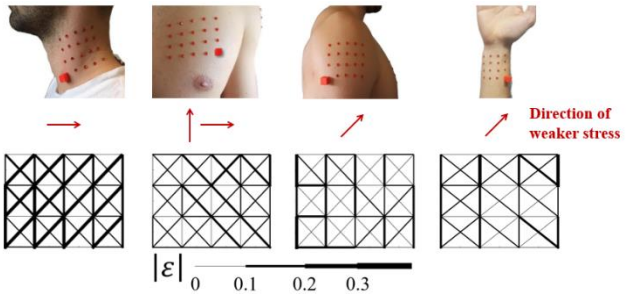

Fig. 6: Meta-representation of skin deformation for the four considered body regions and for all the gestures in Fig. 2. The arrows indicate the direction of weaker stress.

III. Mechanical and Electromagnetic Model of Stretched Antenna

The outcomes of the experimental mechanical analysis are now exploited to numerically evaluate the deformations and the corresponding degradation of the electromagnetic performance of three layouts of antennas that are typically used in epidermal applications, namely: *i*) the ring, *ii*) the split ring and *iii*) the meandered dipole (Fig. 7). For all the cases the external size is included within $3\text{ cm} \times 3\text{ cm}$ [15] square that is a typical footprint of a square plaster.

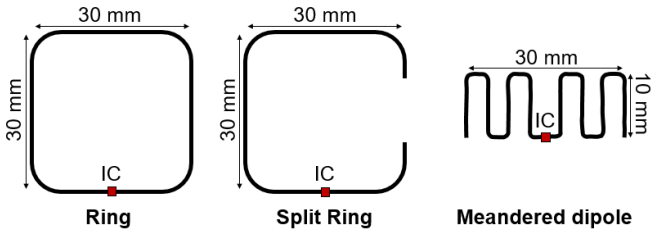

Fig. 7: Reference epidermal antenna layouts to evaluate and compare deformations.

A. Mechanical model

The structural and electromagnetic models are based on a plane surface (skin) with the antenna placed in the middle (Fig. 8). The surface is rigidly constrained at one end and an enforced displacement is applied to the opposite side. For the next analysis, the above antennas are stimulated with the maximum strain $\varepsilon = 0.3$ that was derived by experimental campaign in the previous Section.

Only positive displacements are considered in order to avoid buckling phenomena. The applied displacement stretches the surface and the antenna follows the deformation accordingly.

The antenna layout is assumed to be placed onto a rectangular $6\text{ cm} \times 4.5\text{ cm} \times 0.08\text{ mm}$ slab (elastic module $E = 10^6$ Pa, Poisson coefficient $\upsilon = 0.45$) emulating the human skin [16]. To reproduce the worst case of deformation in the mechanical simulation, the antennas, that are typically fabricated by an inkjet-printed conductor or by means of a thin copper wire, are here preliminary assumed to be made of the same material of the skin substrate. This choice ensures a conservative scenario in which the skin strain is seamless transmitted to the antenna

and therefore its deformation is maximized. A true wire antenna model will be instead considered later on for the electromagnetic analysis.

By using a mechanical FEM solver (DS - Solidworks Simulation [17]), the antenna layout is hence subjected to $\Delta l = 10$ mm linear elongation (derived from the maximum strain) along several angular directions $\phi_n = n\,\pi/6$. For simulation opportunity, the stimulus is kept fixed while the antennas are incrementally rotated by ϕ_n angles (Fig. 8). The corresponding lumped *stiffness*, *i.e.* the ratio between the applied strength and the relative elongation [18], is evaluated as

$$K^D(\phi) = \left(\sum_{i=1}^{n} R_{v1,i}(\phi) - \sum_{j=1}^{n} R_{v2,j}\right)/\Delta l, \qquad (2)$$

where $R_{v1,i}$ and $R_{v2,j}$ are the constraint reactions of the whole system and of the skin-substrate without the antenna, respectively. Small values of K^D at some given angles indicates a low sensitivity of the antenna stiffness to the imposed strain along those angles.

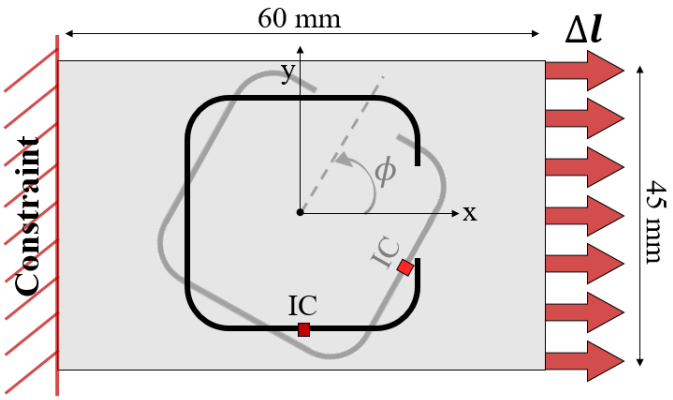

Fig. 8: Scheme of the mechanical stimulus enforced to the epidermal antenna layout. The linear elongation $\Delta l = 10$ mm along angle ϕ_n is derived by the maximum strain obtained by experimental measurements.

B. *Electromagnetic Model*

The so obtained deformed antennas are then analysed at 870 MHz by the electromagnetic solver CST Microwave Studio [19]. The antenna is now more realistically assumed to be made of thin (0.08 mm radius) insulated copper wires, as in the real life. Antennas are placed over a 20 cm × 20 cm multi-layered model of human body: 60 mm of muscle (relative permittivity $\varepsilon_r = 55.1$ and electrical conductivity $\sigma = 0.90\,\mathrm{S/m}$), 10 mm of fat ($\varepsilon_r = 5.5$, $\sigma = 0.05\,\mathrm{S/m}$) and 1 mm of skin (same parameters of the muscle). For comparison, let's denote with G_0 the realized gain[1] of the unstretched antenna, that is assumed to be perfectly matched to the microchip impedance. Mechanical strain is expected to produce a change of the realized gain (ϕ_n), and accordingly a reduced read distance. The electromagnetic performance parameter is hence the variation $\Delta G(\phi_n)$ of the broadside realized gain (namely along the direction that is orthogonal to the skin) w.r.t. that of the unstressed antenna configuration:

$$\Delta G(\phi_n) = G_{\tau,dB}(\phi_n) - G_{\tau 0,dB} \qquad (3)$$

In general, values of ΔG close to 0 dB indicate a minor sensitivity of the antenna to the strain along the specified angles.

Overall, the epidermal antenna is as more tolerant to the applied strain as soon as the stiffness is closer to zero and the differential gain approaches 0 dBi.

C. *Analysis of Combined results*

Fig. 9 combines both the resulting mechanical and electromagnetic behaviour of the deformed epidermal antennas. A polar representation is adopted, simultaneously resuming the stiffness and the variation of the broadside gain corresponding to each direction of strain application. The deformed shape and the resulting electric currents are reported as well.

It is worth observing that the three antennas exhibit different responses and that the critical strain directions for stiffness and gain degradation are different.

Tab. I summarizes the worst variation (ΔG_{max}) of the radiation gain (w.r.t. the un-stretched reference antenna) and the corresponding angles of the applied 0.3 strains, as well as the largest stiffness. The ring looks the most insensitive layout to deformation regarding the gain, with a nearly isotropic response. High stiffness instead appears for a mechanical stimulus along $\phi_n = n\pi/2$ that instead does not produce gain degradation. The split-ring layout, instead, exhibits a rather un-isotropic sensitivity to mechanical and electromagnetic indicators. In particular there are some strain directions $\phi_n = \frac{2\pi}{3} + n\pi$ that are simultaneously critical for both the gain reduction ($\Delta G = -3$ dB) as well as for the relative stiffness. Finally, the maximum stiffness of the meandered dipole is an order of magnitude lower than the previous cases, and hence, as expected, it is the most mechanically resilient configuration. However, its realized gain is 5 dB lower than the other layouts due to the higher power loss that is induced in the tissues by the meander sections where the antenna currents are in phase opposition.

Overall, the maximum electromagnetic degradation of the considered deformed antennas w.r.t. the undeformed ones may exceed 3 dB. Practically speaking, this value means a reduction of the read distance of about 30% and, depending on the application, it may produce a not negligible degradation of the link robustness and reliability (ex. 70 cm instead of 1 m).

[1]The Realized Gain is the product between the gain and the power transmission coefficient [23], taking into account both the mismatch of the antenna input impedance w.r.t. the microchip and the reduced harvested power.

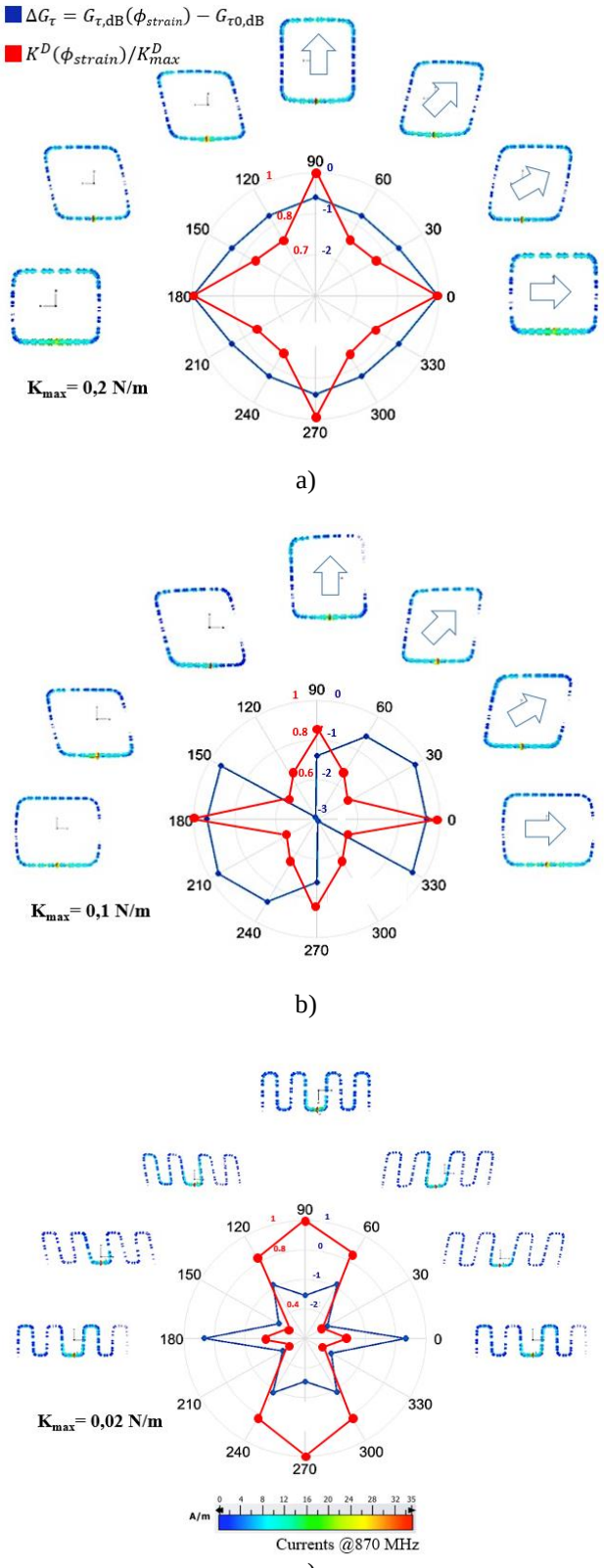

Fig. 9: Combined mechanic deformation and electromagnetic responses at 870 MHz of three typical epidermal antennas: a) ring, b) split-ring and c) meandered dipole. Arrows indicate the direction of the strain applied to the mathematical antennas.

IV. Experimental Corroboration

The outcomes of the numerical analysis are here corroborated by experimental tests involving a true epidermal antenna (Fig. 10) derived from [10]. The antenna is made of a thin copper wire (radius 80 μm) that is shaped along a square split-ring layout (size: 3 cm by 3 cm) provided with a local meander path to electromagnetically couple with a small aluminium loop exciter. This is in turn connected to the Impinj Monza R6 [20] IC. The antenna conductor lays down an ultrathin (50 μm) flexible and elastic PVC (Polyvinyl Chloride) medical grade membrane (Fixomull® Transparent) for comfortable bond with the skin.

The epidermal antenna was placed over the body (Fig. 11) in the same positions as in Fig. 2. Without loss of generality, measurements were performed in case of normal skin hydration. Due to the high natural electric loss of the human body, the possible effect of sweat on the radiation performance of this kind of epidermal antenna can be considered as a second-order effect and we do not expect a significant change of results. The broadside realized gain was measured by the Voyantic Tagformance station during different body gestures, according to the turn-on power method [21]. For this purpose, the broadband interrogating antenna was kept at a fixed distance ($d = 40$ cm) from the skin portion hosting the antenna by the help of a laser meter. Moreover, for each poses of the body, the orientation of the reader's antenna was manually adjusted so that the laser always focuses on the centre of the epidermal tag, thus roughly keeping the two antennas aligned. Denoting with P_{to} the minimum output power emitted by the reader's unit so that the tag starts responding, the realized gain is derived from the Friis formula [22] as:

$$G_\tau = \left(\frac{4\pi d}{\lambda}\right)^2 \frac{p_C}{P_{to} G_R \eta_P} \alpha \qquad (3)$$

where η_P is the polarization loss factor, G_R the reader antenna gain, p_C the chip sensitivity and $\alpha = 2$ dB the attenuation of the cable. The polarization loss factor is assumed as η_P=1 (aligned antennas).

TABLE I: Summary of the response (worst values) of typical epidermal antennas to a 0.3 strain at various directions

	Max Gain of undeform. ant. [dB]	*Worst ΔG of deform. ant.* [dB]	*Strain angles of worst ΔG* [°]	*Worst Stiff. of deform. ant.* [N/m]	*Strain Angles of worst Stiff.* [°]
Ring	-13.0	-0.5	/	0.2	0, 90, 180, 270
Split ring	-13.0	-3	120, 300	0.1	0, 180
Meander Dipole	-18.3	-2.0	90, 270	0.02	90, 270

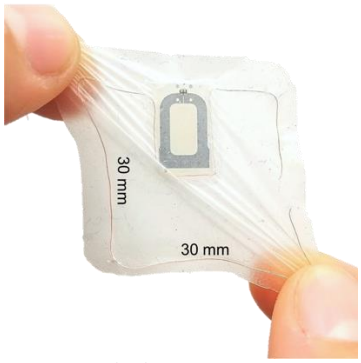

Fig. 10: Reference prototype of a flexible and stretchable split-ring epidermal tag made by a thin copper wire as main radiator, an aluminium coupling loop connected on PET connected the Impinji Monza R6 chip, as exciter and a breathable polyurethane membrane.

Fig. 11: The stretchable epidermal antenna placed on the neck, wrist, chest and deltoid of a volunteer (here in rest position).

As the numerical model was related to a simplified (planar) phantom, that hence differs from the morphological in-homogeneity of the human body, an absolute comparison with the numeric results is meaningfulness. Thus, experimental results are reported in differential values with respect to the maximum gain of the antenna in rest conditions, so that the overall change of the performance can be compared with the corresponding values predicted by the radio-mechanical model. An example of measured realized gain for the deltoid case in a wide frequency band is shown in Fig. 12.

Deformation produces both a frequency shift as well as a gain variation that, in some cases (gesture *a*), is positive (improvement w.r.t. rest) but it is generally negative down to -4 dB. Fig. 13 resumes the measurements at 870 MHz for all the considered positions and gestures. Such indicator is comprised in the range $-5\ \text{dB} < \Delta G_\tau < 3\ \text{dB}$, with an average value of $\Delta G_{\tau,av} = -0.9\ \text{dB}$. The worst case ($\Delta G_{\tau,worst} = -5\ \text{dB}$) corresponds to the gesture *c* of the wrist. It is worth noticing that, due to the huge deformation of the wire radiator during that gesture, the tag no longer responds at 870 MHz for the gesture *b* of wrist. In this case, a closer look to the results showed a frequency shift of the gain peak from 900 MHz to 920 MHz.

Overall, in spite of the simplified electro-mechanical model that only accounted for two-dimensional dilations of the epidermal antenna, and despite the shadowing and scattering effects produced by the *moving* portions of the body segments (like the head and the hand) that were not included in the simulations, the measurement campaign looks nevertheless to reasonably confirm the numerical analysis of the previous Section which predicted a worst case of gain degradation $\Delta G_\tau = -3\ \text{dB}$.

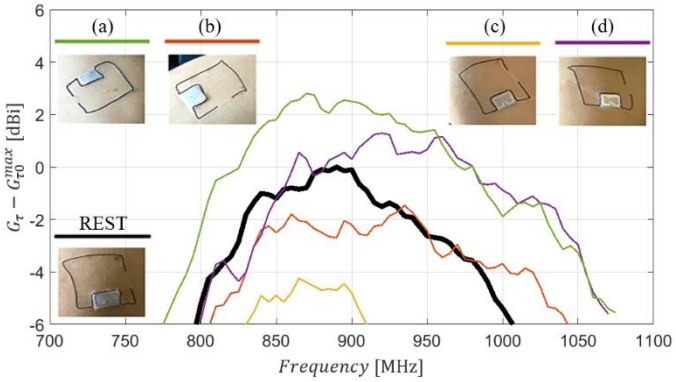

Fig. 12: Example of measured realized gain (along the observation direction orthogonal to the skin) of open-ring epidermal tag placed onto the deltoid for the gestures in Fig. 2. Gain values are normalized ($G_{\tau,\text{dB}} - \max\{G_{\tau 0,\text{dB}}(f)\}$) by the maximum realized gain for case of body at rest.

Position	Rest	(a)	(b)	(c)	(d)	(e)	(f)
Neck		$\Delta G_\tau = -3$ dB	$\Delta G_\tau = 1$ dB	$\Delta G_\tau = -3$ dB	$\Delta G_\tau = -3$ dB	$\Delta G_\tau = -1$ dB	$\Delta G_\tau = 1$ dB
Wrist		$\Delta G_\tau = 0.5$ dB	Not readable	$\Delta G_\tau = -5$ dB	$\Delta G_\tau = -0.5$ dB	\	\
Chest		$\Delta G_\tau = -1$ dB	$\Delta G_\tau = -1$ dB	$\Delta G_\tau = -1$ dB	$\Delta G_\tau = 2.5$ dB	\	\
Deltoid		$\Delta G_\tau = 3$ dB	$\Delta G_\tau = -1.5$ dB	$\Delta G_\tau = -4$ dB	$\Delta G_\tau = 0$ dB	\	\

Fig. 13: Resume of the deformations and of the corresponding variations of the realized gains at 870 MHz when the reference epidermal tag is applied on the same parts of the body as in Fig. 11 and for the gestures in Fig. 2.

V. Conclusion

A numerical and experimental campaign has quantified the deformation of the human skin due to common gestures. The corresponding mechanical and electrical behaviour of typical epidermal UHF antennas has been resumed in a combined representation showing that constraints over low stiffness and insensitivity of radiation gain to deformation could be not always compatible. Among the several considered body regions, the neck is the most challenging site as it produces relevant stretching during common gestures that may simultaneously induce fatigue to the antenna and non-negligible degradation of read-range.

From a design perspective, antenna deformation arising from the natural body gestures, definitely translates into an additional margin of at least 3-4 dB in the antenna optimization in order to guarantee a reliable communication link with an epidermal tag in random body gestures, especially when a fixed reader is involved, like a gate.

Finally, the peculiar representations of strain, stiffness and gain degradations permit to understand the most appropriate antenna orientation and moreover could be used as an aid for the efficient design of new generation of deformation-insensitive antenna layouts.

ACKNOWLEDGMENT

Work funded by Lazio Innova, project SECOND SKIN, Ref. 85-2017-14774.

VI. REFERENCES

[1] J. A. Rogers, R. Ghaffari and D. H. Kim, Stretchable Bioelectronics for Medical Devices and Systems, Springer, 2016.

[2] Y. Liu, M. Pharr and G. A. Salvatore, "Lab-on-Skin: A Review of Flexible and Stretchable Electronics for Wearable Health Monitoring," *ACS Nano*, vol. 11, no. 10, pp. 9614-9635, 2017.

[3] T. R. Ray and et al., "Bio-Integrated Wearable Systems: A Comprehensive Review," *Chemical Review*, vol. 119, no. 8, pp. 5461-5533, 2019.

[4] M. A. Ziai and J. C. Batchelor, "Temporary On-Skin Passive UHF RFID Transfer Tag," *IEEE Transactions on Antennas and Propagation*, vol. 59, no. 10, pp. 3565-3571, 2011.

[5] S. R. Krishnan and et al., "Wireless, Battery-Free Epidermal Electronics for Continuous, Quantitative, Multimodal Thermal Characterization of Skin," *Small Journal*, vol. 14, no. 47, pp. 1-13, 2018.

[6] S. Amendola, G. Bovasecchi, A. Palombi, P. Coppa and G. Marrocco, "Design, Calibration and Experimentation of an Epidermal RFID Sensor for Remote Temperature Monitoring," *IEEE Sensors Journal*, vol. 16, no. 9, pp. 7250-7257, 2016.

[7] S. Amendola, S. Milici e G. Marrocco, «Performance of Epidermal RFID Dual-loop Tag and On-skin Retuning,» *IEEE Transactions on Antennas and Propagation*, vol. 63, n. 8, pp. 3672-3680, 2015.

[8] S. Amendola, G. Bovasecchi, A. Palombi, P. Coppa and G. Marrocco, "Design, Calibration and Experimentation of an Epidermal RFID sensor for remote Temperature Monitoring," *IEEE Sensors Journal*, vol. 16, no. 19, pp. 7250-7257, 2016.

[9] S. Amendola, S. Milici and G. Marrocco, "Performance of Epidermal RFID Dual-loop Tag and On-skin Retuning," *IEEE Transactions on Antennas and Propagation*, vol. 63, no. 8, pp. 3672-3680, 2015.

[10] F. Amato, C. Miozzi, S. Nappi and G. Marrocco, "Self-Tuning UHF Epidermal Antennas," in *IEEE RFID-TA Conference*, Pisa, (IT), 25-27 Sept. 2019.

[11] S. Y. Y. L. Leung and D. C. C. Lam , "Performance of Printed Polymer-Based RFID Antenna on Curvilinear Surface," *IEEE Transactions on Electronics Packaging Manufacturing*, vol. 30, no. 3, pp. 200-205, 2007.

[12] G. Diotallevi, C. Miozzi, M. Cirelli, P. P. Valenti and G. Marrocco, "Radio-Mechanical Model of Epidermal Antenna," in *IEEE FLEPS Conference*, Glasgow, Scotland (UK), 2019.

[13] L. Piegl and W. Triller, The NURBS Book (2nd ed.), Berlin: Springer, 1997.

[14] S. M. Hashemi-Dehkordi and P. P. Valentini, "Comparison between Beizer and Hermite cubic interpolants in elastic spline formulations," *Acta Mechanica*, vol. 225, no. 6, pp. 1809-1821, 2014.

[15] C. Miozzi, S. Nappi, S. Amendola, C. Occhiuzzi and G. Marrocco, "A General-purpose Configurable RFID Epidermal Board with a Two-way Discrete Impedance Tuning," *IEEE Antennas and Wireless Propagation Letters*, vol. 18, no. 4, pp. 684-687, 2019.

[16] H. Jeong and et al., "NFC-Enabled, Tattoo-Like Stretchable Biosensor Manufactured by "Cut-and-Paste" Method," in *IEEE EMBC*, Seogwipo, South Korea, 11-15 July 2017.

[17] Solidworks, Dassault Systems, 2016. [Online]. Available: https://www.solidworks.com/it. [Accessed 22 October 2019].

[18] E. Baumgart, "Stiffness--an unknown world of mechanical science?," *Injury*, pp. S-B-14-S-B-23, 2000.

[19] CST Studio Suite, Dassault Systems, 2018. [Online]. Available: https://www.3ds.com/products-services/simulia/products/cst-studio-suite/. [Accessed 22 October 2019].

[20] Impinj Monza R6, [Online]. Available: https://support.impinj.com/hc/en-us/articles/202765328-Monza-R6-Product-Brief-Datasheet. [Accessed 22 October 2019].

[21] P. V. Nikitin and R. K. V. S. , "Theory and measurement of backscattering from RFID tags," *IEEE Antennas and Propagation Magazine*, vol. 48, no. 6, pp. 212-218, 2006.

[22] C. A. Balanis, Antenna Theory Analysis and Design, New York: Wiley, 1997.

[23] D. Dobkin, The RF in RFID, Burlington: Elsevier, 2012.

Carolina Miozzi - received the M.Sc. degree in medical engineering from the University of Rome Tor Vergata in 2017, where she is currently pursuing the Ph.D. degree in electronics engineering. Her research interests include on-skin antennas and through-the-body wireless communication systems for smart health monitoring and detection of biophysical parameters. She is currently researching on the development of a wireless power transfer and transcutaneous telemetry system for the control of robotic limb prostheses, using EMG-sensors implanted subcutaneously.

Gabriele Diotallevi - He received the M.Sc. degree in Medical Engineering in 2018. After an Internship at The Robert Group company in Los Angeles, he is currently involved as Product Specialist in two Hospitals of Rome. This job involves training of personnel for the use of new Electronic Health Record and Patient Charts.

M. Cirelli - received M.S. degree in Mechanical Engineering from the University of Rome Tor Vergata in 2016. Currently he is finalizing his Ph.D. in Design Manufacturing and Operations Engineering at University of Rome Tor Vergata working on innovative methods for simulating the dynamics of flexible bodies. He is also an Adjunct Professor of Applied Mechanics at University of Niccolò Cusano. His research interests are reverse engineering, multibody dynamics, compliant mechanisms, vibration-dampers, structural analysis, and virtual prototyping.

Pier Paolo Valentini - received M.S. in Mechanical Engineering in 2000 and Ph.D. in Design of Mechanical Systems in 2004 from University of Rome Tor Vergata. Currently, he is Associate Professor of Applied Mechanics and teaches the courses of Virtual Prototyping and Bioprosthesis at the Dept. of Enterprise Engineering of the University of Rome "Tor Vergata". He chairs the Laboratory of Virtual Prototyping and Simulation. His research interests are computational mechanics, virtual prototyping, dynamics and structural simulations, biomechanics and innovative computer-aided methodologies. He is author of more than 140 papers on referred Journals and 3 patents. He has coordinated more than 50 research projects funded by both national and international institutions and industries.

Gaetano Marrocco - received the Laurea degree in electronic engineering and the Ph.D. degree in Applied electromagnetics from the University of L'Aquila, Italy, in 1994 and 1998, respectively.
He is a Researcher with the University of Rome Tor Vergata from 1994 to 2014, an Associate Professor of electromagnetics from 2013 to 2017, a Guest Professor with the University of Paris-Est Marne la Vallèe in 2015, and he is Full Professor at the University of Roma Tor Vergata since 2018, where he currently serves as the Director of the Medical Engineering School and chair of the Pervasive Electromagnetics Lab. His research is mainly directed to the modeling and design of broadband and ultrawideband antennas and arrays as well as of sensor-oriented miniaturized antennas for biomedical engineering, aeronautics and radiofrequency identification (RFID). During the last decade, he carried out pioneering research on the wireless-activated sensors, and in particular, on epidermal electronics, contributing to move from the labeling of objects to the passive sensor networks in the Internet of Things Era.
Prof. Marrocco is the Co-Founder and the President of the University spin-off RADIO6ENSE that active in the short-range electromagnetic sensing for Industrial Internet of Things, smart manufacturing, and automotive and physical security. He serves as an Associate Editor for the IEEE JOURNAL OF RADIOFREQUENCY IDENTIFICATION. He is the Chair of the Italian Delegation URSI Commission D Electronics and Photonics. He was the Chair of the Local Committee of the V European Conference on Antennas and Propagation in 2011, the TPC Chair of the IEEE-RFID TA in Nice, France, and the TPC Track-Chair of the 2016 IEEE Antennas and Propagation International Symposium and the IEEE-RFID 2018 USA. He was a member of the IEEE Antennas and Propagation Society Awards Committee.